Catalysis Letters Vol. 107, Nos. 3–4, March 2006 (© 2006)
DOI: 10.1007/s10562-005-0015-5

Scanning Tunneling Microscopy (STM) at High Pressures. Adsorption and Catalytic Reaction Studies on Platinum and Rhodium Single Crystal Surfaces

Max Montano[a,b], David C. Tang[a,b], and Gabor A. Somorjai[a,b,*]

[a]*Department of Chemistry, University of California, Berkeley, CA 94720, USA*
[b]*Materials Science Division, Lawrence Berkeley National Laboratory, Berkeley, CA 94720, USA*

Received 12 September 2005; accepted 14 December 2005

In this paper, we review the experimental results that were obtained using our high pressure–high temperature STM system (HP/HT STM) for studies of gas adsorption in a broad pressure range. Measurements are carried out in equilibrium with the gas phase. We discovered ordered surface structures of adsorbates that do not exist at low pressures. It appears that small increases in coverage due to increased ambient pressures cause ordering due to repulsive adsorbate–adsorbate interactions. Adsorption isotherms, one of the oldest fields of surface thermodynamics, can be revisited using HP/HT STM to obtain molecular surface structures and surface phase diagrams as the gas pressure is altered.

KEY WORDS: adsorption studies by STM; catalytic reaction by STM; platinum and rhodium crystal surfaces.

1. Introduction

To obtain the surface structures of atoms and adsorbed molecules in equilibrium with the gas or liquid at the interface has been the dream of many surface scientists. Low energy electron diffraction (LEED) [1,2] or ion scattering [3] experiments carried out to obtain surface structures can only be performed at low ambient pressures because of the high scattering cross sections of both electrons and ions. Grazing angle X-ray diffraction [4] using high intensity tunable X-rays from a synchrotron shows promise for surface structure determination of atoms and molecules in the adsorbed monolayer, monitoring substrate restructuring at high pressures. Thus far, however, it has rarely been employed for these types of studies. Experiments in our laboratory with the scanning tunneling microscope (STM) that was built to operate at high pressures and temperatures as well as in ultra high vacuum (UHV) [5] have shown for the first time that atomic and molecular resolution can be obtained over a ten order of magnitude pressure range. The stability of our instrument is such that one can scan the same area as the pressure is being altered. Unfortunately, changes in temperature cause thermal drift and thus scanning the same area while temperature is varied is out of our reach at the present time.

In this paper, we review the experimental results that were obtained using our high pressure-high temperature STM system (HP/HT STM) for studies of gas adsorption in a broad pressure range. Measurements are carried out in equilibrium with the gas phase. We discovered ordered surface structures of adsorbates that do not exist at low pressures. It appears that small increases in coverage due to increased ambient pressures cause ordering due to repulsive adsorbate–adsorbate interactions. Adsorption isotherms, one of the oldest fields of surface thermodynamics, can be revisited using HP/HT STM to obtain molecular surface structures and surface phase diagrams as the gas pressure is altered.

Catalytic surface reactions can also be studied by the HP/HT STM system. While the reaction turnover is monitored by a differentially pumped mass spectrometer the surface is scanned at a 100 Å/ms rate. Our studies of ethylene hydrogenation and cyclohexene hydrogenation/dehydrogenation indicate that during reaction turnover the adsorbed monolayer is mobile on the catalytically active metal surfaces (platinum and rhodium). Thus STM is capable of providing surface dynamic data under reaction conditions that has not been available so far. Such surface mobility appears to be the necessary requirement for catalytic activity. Upon the introduction of carbon monoxide, a poison for these catalytic reactions, ordered surface structures form and the catalytic reaction stops. It appears that the mobility of adsorbates frees up active sites where continued catalytic turnover can occur. When these sites are blocked by immobile adsorbates the reaction is inhibited. In this review we shall also briefly describe the newly constructed ultra high pressure/ultra high temperature STM (UHP/UHT STM) [6] that is capable of reaching 30 atm and over 600 K to extend our range of studies of molecular adsorption isotherms and heterogeneous catalytic reactions.

* To whom correspondence should be addressed.
E-mail: somorjai@socrates.berkeley.edu

2. The high pressure/high temperature STM instrument

2.1. Apparatus

The system consists of three sections connected by a magnetic transfer arm, the UHV sample preparation chamber, the STM analysis chamber and a small load lock. The load lock allows us to transfer tips and samples to and from the system without having to vent either one of the other chambers. The entire system is connected to a 260 l/s turbomolecular pump that can be used to pump any or all three parts of the apparatus.

2.1.1. UHV chamber

The UHV portion of the system is used for sample preparation and characterization. It is a standard Varian surface analysis chamber equipped with Auger electron spectroscopy (AES), quadrupole mass spectrometry (QMS), argon and oxygen ion sputtering, as well as electron beam heating. A Thermionics Northwest sample manipulator is attached to the top of the chamber on a 6 inch flange and allows for X, Y, Z and θ maneuverability of the sample. During annealing, the sample holder is held in contact with a copper block that is cooled by copper coil. N_2 gas, which is flowed through a dewar filled with liquid N_2, passes through the coil creating a heat sink. Sample temperatures up to $\sim$1350 K can be reached. The UHV chamber is pumped by the turbomolecular pump, a 200 l/s ion pump, and a liquid nitrogen cooled titanium sublimation pump. The base pressure during operation is $\sim 3\times10^{-10}$ Torr.

2.1.2. STM chamber

The STM portion of the apparatus is a custom built system from RHK technologies. The STM stage is mounted horizontally on an 8-inch flange connected to the rear of the chamber. The chamber can be isolated from the rest of the system by gate valves. This allows introduction of pressures up to slightly above one atmosphere into the STM chamber while the rest of the system remains at UHV. The entire volume of the chamber is approximately 10 L and it is connected via a 3.5 ft long 1/4 inch diameter stainless steel tube to a leak valve allowing introduction of low pressures of gas from the STM chamber into the UHV chamber for analysis with the mass spectrometer. The chamber has three additional valves connected to gas cylinders as well as one attached to a liquid sample reservoir. In the case of the liquid sample, a direct drive mechanical pump is connected for freeze-pump-thaw purification of our samples. A standard ion gauge and two Baratron pressure gauges are also in the chamber allowing pressure reading ranging from 1×10^{-10} Torr to 1000 Torr. The chamber is pumped by the turbomolecular pump as well as a 60 l/s ion pump.

2.1.3. Scan head

The microscope itself is a beetle type design commercially available from RHK technologies. The STM stage is mounted on three Viton rings to provide secondary vibrational isolation from the rest of the system. The stage can be cooled during sample heating by a water line running through the rear of the system and connected to the stage by a copper braid. During introduction of high pressures of gases, the tip can be brought back out of range using solely the scan piezo allowing for imaging of the same portion of the sample. In order to heat our sample in the presence of high pressures of potentially reactive gases, the standard electron beam heater has been replaced by a 150 W, tungsten filament, halogen filled, quartz projector bulb. The bulb provides radiative heating without making mechanical contact. The bulb can be raised into position so it is directly below the sample providing the most efficient heating possible, reaching sample temperatures up to 400 K. Due to the expansion of the sample as it is heated, it is generally very difficult to remain in the same position on the sample over a range of temperatures. As a result, many portions of the sample must be imaged to gather a representative image of the surface structure.

2.2. Sample preparation

Our experiments were performed on metal single crystals of platinum and rhodium of (111) orientation. Once crystals are cut within 1° of the (111) orientation, the samples are polished using diamond paste of decreasing grit size down to 1/4 micron. After sequentially sonicating in methanol and acetone, the sample is mounted and inserted in the chamber. Prior to each experiment the sample is sputtered with oxygen and/or argon ions for 10 min followed by annealing in vacuum at 1123 K for 10 min in the case platinum and 923 K for 2 min in the case of rhodium. Just prior to transferring the sample to the STM chamber, the sample is flashed to its annealing temperature for 1 min.

2.3. Tip preparation

Tungsten was chosen as a tip material due to its rigidity, ease of etching and ability to provide stable imaging at room temperature and high pressures of the gases we are using. Our tips were prepared using etched 0.010 in. tungsten wire. Our etching procedure uses a platinum loop of 8 mm inner diameter dipped in a 2 M KOH solution forming a KOH film across the loop. The W wire is then inserted through the platinum loop and the platinum and W wires are connected to an external voltage supply. Tips are etched with 3 V bias until the wire is almost completely etched through. The wire is then flipped and the final etching is completed using a 1 V bias. The bottom portion of the wire eventually drops into a properly placed cup and after rinsing with de-ionized H_2O and acetone it is inserted into the

chamber. This procedure generally produces reliable and robust tips. Approximately 1 in 3 is capable of providing molecular resolution.

2.4. STM capabilities

Our STM can provide atomic resolution over a large range of pressures and temperatures. For example in UHV the system can provide atomic resolution of a single crystal metal substrate such as platinum (111) (figure 1a). As the pressure is increased imaging can become slightly more difficult. The tip can become unstable as molecules adsorb and desorb, also the addition of gases allows for vibrations from the chamber to more easily be transferred to the sample. Despite this, molecular resolution can routinely be obtained at high pressures (figure 1b). As temperature is increased imaging of surface structure also becomes more difficult. Thermal drift becomes much more of a problem, and great care must be taken to ensure thermal stability. In addition the mobility of the adsorbates and potentially the substrate atoms can increase to the point that molecular structure cannot be observed.

3. The new ultra high pressure/ultra high temperature STM (UHP/UHT STM) system

While the research we have done with our current HP/HT STM has been invaluable in bridging the pressure gap between traditional ultra high vacuum STM studies and high pressure adsorption and reaction studies, extending the pressure and temperature ranges of our STM studies opens up many new research opportunities. Many industrial processes are carried out at tens of atmospheres and at temperatures near 1000 ° C. Our current system capabilities are about an order of magnitude lower in both temperature and pressure. We have been constructing an ultra high pressure/ultra high temperature scanning tunneling microscope (UHP/UHT STM) in our laboratory that has many improvements over the current system [6].

3.1. Higher pressures and temperatures

With our new system we have increased range of operation. In pressure, the new UHP system can be employed at a maximum pressure of 30 atm, while still being capable of UHV studies. Maximum operating temperatures have increased to 1273 K in vacuum and 623 K at high pressure. The higher pressure is achieved by the design and fabrication of a custom high pressure cell enclosed in the STM chamber. The increase in operating temperature is accomplished by replacing the light bulb with a custom designed button heater directly behind the sample.

3.2. Smaller chamber volume

One of the major limitations of our current system is its inability to detect products in high pressures of background gases. Since our means of detection is a mass spectrometer, unless significant fractions of reactant gases have been converted to products, then they are below our detection limits. Our approach to remedy this problem is the reduction of the size of the reaction chamber. While the volume of the original chamber was on the order of 10,000 cm^3, the new system has a reaction chamber of less than 10 cm^3: a reduction in volume of more than 3 orders of magnitude. Also instead of a batch reactor, the new design is a flow cell eliminating diffusion problems during reaction studies. Additional benefits of the smaller volume also include the consumption of smaller amounts of material as well as having a smaller surface area for the adsorption of gases to the chamber walls.

3.3. Less mechanical contact to the surrounding chamber

A final major improvement of the new STM system is that it was designed to limit the mechanical contact of the ultra high pressure cell with the rest of the system during imaging. To accomplish this, the UHP cell is contained within a UHV chamber. During sample/tip transfer the UHP cell can be secured on a docking

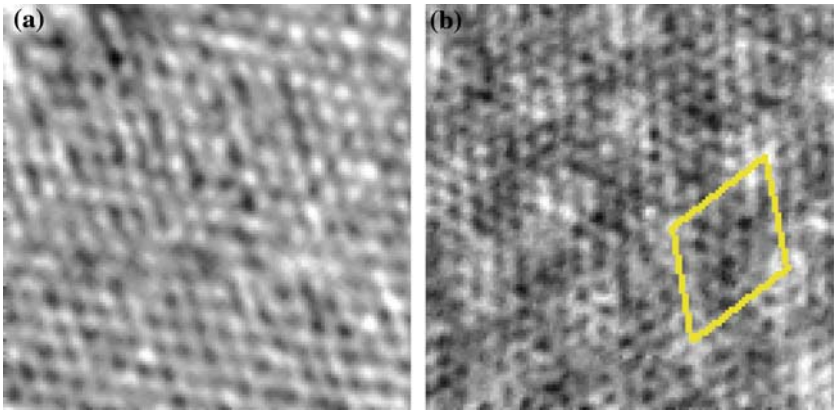

Figure 1. (a) 50 Å×50 Å image of Pt(111) in vacuum at 300 K. Atomic periodicity is resolved. (b) 50 Å×50 Å image of Pt(111) exposed to 5 Torr CO at 300 K. ($\sqrt{19}\times\sqrt{19}$) R23.4° unit cell is marked. Individual CO molecules are not always resolvable in reaction studies.

scaffold providing a rigid stage during opening and closing of the cell. During imaging however, the scaffold can be lowered and the cell is hung from 3 springs. The result is that the high frequency vibrations from the chamber are not coupled to the UHP cell. Also, special care was taken during design and material selection to ensure that no resonating body within the cell had a frequency lower than 1 kHz. Thus low frequency vibrations do not excite the UHP cell. The result is a robust system potentially capable of imaging while turbomolecular pumps pump on the surrounding chamber.

4. Results

4.1. High pressure gas adsorption studies

Various types of gaseous species have been studied at high pressures in equilibrium with noble metal surfaces using STM in our group. Among these systems are CO, NO and CO + NO on Rh(111) and CO and various cyclic C_6 species on Pt(111). From these studies we are able to put together surface phase diagrams that truly emphasize the capability of STM to obtain molecular level surface structural information at high pressures that cannot be obtained in any other way.

4.1.1. CO adsorption on Rh(111) [7]

When Rh(111) is exposed at 300 K to pressures of CO ranging from 10^{-8} Torr up to 700 Torr, several surface structures are observed as a function of pressure. Exposing the crystal to 5×10^{-8} Torr of CO results in the formation of a (2×) overlayer of CO shown in figure 2a. Increasing the back pressure above 10^{-7} Torr induces the formation of a new structure with a periodicity of ($\sqrt{7}\times\sqrt{7}$) R19° (figure 2b). This new structure remains stable up to ~1 Torr at which point it converts to a (2×2) (figure 2c). The (2×2) is the only structure we observed up to pressures of 700 Torr.

4.1.2. NO adsorption on Rh(111) [8]

Similar experiments on the (111) crystal face of rhodium were performed using NO as the adsorbate with similarly interesting results. Initial adsorption at pressures of 1×10^{-8} Torr reveals the formation of a (2×2) – 3NO structure (figure 3a) that was previously solved with LEED [9]. This structure is stable and the only structure present up to a back pressure of 0.01 Torr. Above 0.01 Torr however a new structure is observed that has a (3×3) periodicity. The (3×3) structure has a larger corrugation as well as an apparent height of ~0.1 Å higher than the (2×2), suggesting an expansion of the top layer of rhodium atoms. As is shown in

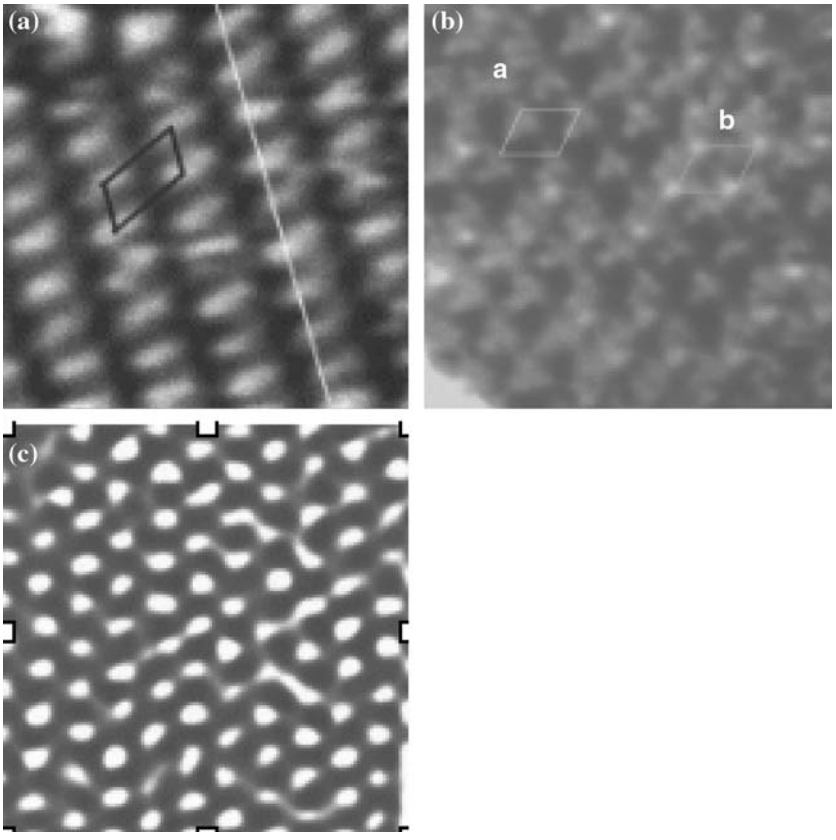

Figure 2. STM images of Rh(111) in the presence of different pressures of CO (a) (2×1) structure of adsorbed CO. The structure is formed by the presence of a CO gas pressure of 5×10^{-8} Torr (b) (Ö7×Ö7) R19° structure observed from pressures ranging from 10^{-7} Torr up to ~1 Torr (c) A 50×50 $Å^2$ image in 700 Torr CO. This image shows the (2×2) pattern observed in the CO pressure range between 5 and 700 Torr.

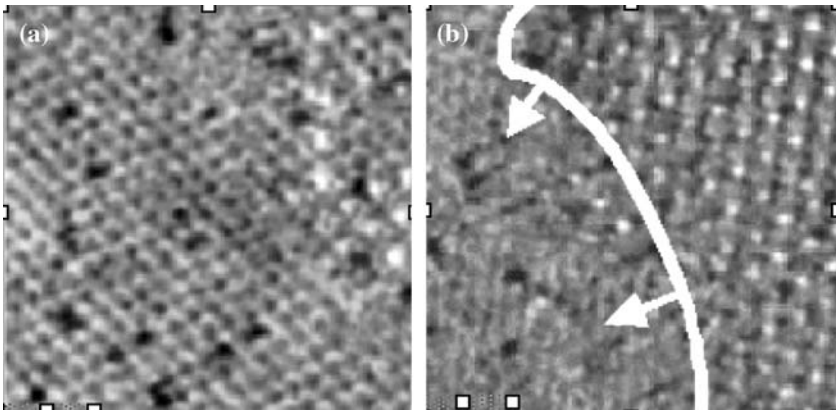

Figure 3. 100 Å×100 Å STM images of Rh(111) taken in 0.03 Torr of NO at 25 °C, showing the phase transition between a (2×2) and a (3×3) structure. (a) taken at 0 s, the majority of the surface shows the (2×2) structure, except for the upper right-hand corner which shows the (3×3) structure. (b) taken at 110 s. the phase boundry has moved across almost half of the image.

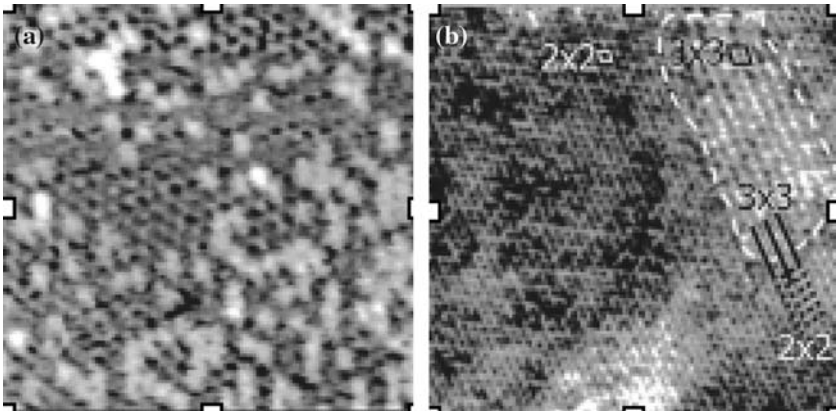

Figure 4. (a) 120 Å×120 Å image taken upon exposure to 0.50 Torr CO and 0.70 Torr NO. A (2×2) pattern, which is characteristic of the (2×2)-3CO structure is observed. The brighter unit cells are due to NO adsorption on the top sites (b) STM image showing formation of the (3×3) structure. The 200 Å×200 Å image was taken in 0.10 Torr CO + 0.32 Torr NO. The brighter, nearly pure NO regions of the surface are the nucleation sites for the formation of the (3×3) structure that is characteristic of high-pressure NO adsorption.

figure 3b, c, the (2×2) converts to the more stable (3×3) over the course of minutes. By repeating the experiment over various temperatures, a phase diagram was constructed that contained a clear phase boundary in which both species were present and stable on the surface. In addition the dynamic behavior of the phase boundary allowed the calculation of an energy barrier for the conversion from the (2×2) to the (3×3) of ~0.7 eV.

4.1.3. NO + CO coadsorption on Rh(111) [10]

To understand the coadsorption of CO and NO on the Rh(111) surface experiments were carried out at ~1 Torr total pressure to investigate both the ability of STM to discriminate between the two adsorbates and the behavior they displayed on the crystal surface when coadsorbed. Indeed it was shown that the molecules are very easy to distinguish from one another, with NO appearing much brighter than neighboring CO molecules. When the surface was initially exposed to 0.50 Torr of CO the (2×2) structure discussed above is observed. Adding 0.15 Torr of NO to the gas mixture results in the appearance of a few bright spots on the surface representing about 1% of the adsorbed molecules. Increasing the NO pressure to 0.70 Torr causes about a quarter of the surface CO molecules to be replaced by adsorbed NO (figure 4a). The appearance of NO does not appear to be random, with sites having a neighboring NO molecule already present, being favored. Monitoring the surface over time, the displacement of one adsorbate with another was observed. Finally, when the clean rhodium surface is sequentially exposed to a gas mixture with the partial pressure of NO two to four times greater than that of CO, segregation of areas that are rich in NO appear (figure 4b).

4.1.4. CO adsorption on Pt(111) [11]

The high pressure adsorption of CO on Pt(111) was studied in the pressure range of 200–700 Torr. It was found that a hexagonal structure with a periodicity of

~12 Å formed under these conditions (figure 5). This was the first time that this structure had been observed at these conditions and it was later proven by Besenbacher et al. [12] to be the ($\sqrt{19}\times\sqrt{19}$) R23.4° structure now known to exist under high pressures. Further studies by Ocko [4] have also shown site specific relaxation of the underlying platinum atom.

4.1.5. *Cyclic C_6 hydrocarbons adsorbed to Pt(111)[13]*

A Pt(111) single crystal was exposed at 300 K to low pressures (2×10^{-6} Torr to 1×10^{-5} Torr) of various cyclic C_6 hydrocarbons including cyclohexane, cyclohexene, 1,3-cyclohexadiene, 1,4-cyclohexadiene, and benzene. At 2×10^{-6} Torr both cyclohexane and cyclohexene form the same structure on the surface (figure 6a, b). Spectroscopic [14] and thermal desorption [15] studies tell us that the species present at room temperature is the partially dehydrogenated π-allyl C_6H_9. The periodicity of ~5.5–6 Å suggests that the structure may in fact be a (2×2), but further studies are necessary to determine the orientation of the underlying platinum lattice. When exposed to 1×10^{-5} Torr of 1,4-cyclohexadiene the platinum surface exhibits a complicated surface structure with long-range periodicity of 150 Å as well as a smaller scale periodicity of about 25 Å (figure 6c). Further research is currently being performed on these systems to determine the actual structures formed by each type of molecule. Both benzene and 1,3-cyclohexadiene form a hexagonal structure of periodicity of ~9 Å suggesting that the 1,3-cyclohexadiene dehydrogenates to benzene in the presence of the platinum catalyst (figure 6d, e). Using large scale defects corresponding to the (110) lattice plane in the case of benzene, the underlying orientation of the platinum was determined. The benzene structure orientation is rotated 30° relative to the platinum. This rotation and the periodicity suggest a ($2\sqrt{3}\times2\sqrt{3}$) R30° structure.

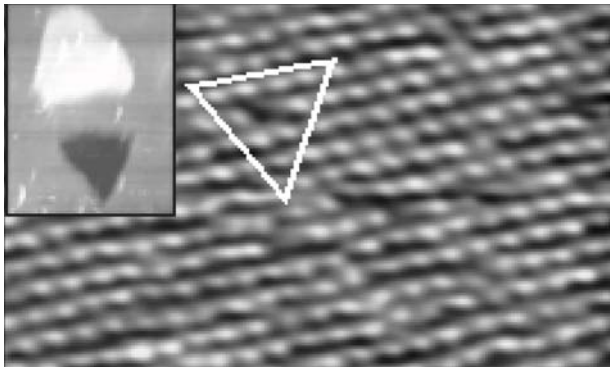

Figure 5. A 270 Å×150 Å STM image obtained in 150 Torr CO and 50 Torr O_2 after annealing at 183 °C. The insert, 1600 Å×2000 Å shows the Moiré patterns alignment to [110] step edges (close-packed row direction).

4.2. *Reaction studies*

Among the most valuable applications of STM is its ability to monitor active catalyst surfaces, providing time-resolved, molecular information under reaction conditions. We have employed our high pressure STM to study the role of surface mobility on the platinum and rhodium catalyzed hydrogenation of ethylene as well as the platinum catalyzed hydrogenation/dehydrogenation of cyclohexene. CO poisoning experiments were also performed on these systems in attempt to fully characterize both the active and inactive catalyst surface.

4.2.1. *Ethylene hydrogenation and poisoning of the catalytic reaction with CO on platinum and rhodium [16]*

Upon adsorption on the (111) crystal faces of platinum and rhodium at 300 K, ethylene has been found to convert irreversibly to ethylidyne(CCH_3) [17]. Although it is very strongly bound to the metal surface its high mobility at room temperature make resolving it with our STM impossible. If the sample is cooled to temperatures near 200 K, however, the mobility can be lowered enough to acquire STM images showing the periodicity of an ordered (2×2) structure [18]. Our studies focus on room temperature ethylene hydrogenation and its poisoning with CO on Pt(111) and Rh(111).

4.2.2. *Ethylene hydrogenation and CO poisoning of the catalytic reaction on Pt(111)*

The platinum surface after the addition of 20 mTorr each of hydrogen and ethylene at 300 K is shown in figure 7a. No surface order can be detected indicating rapid diffusion of the adsorbates. Mass spectrometry confirmed that the catalyst surface was active by detection of gas phase ethane production resulting in a hydrogenation rate of 2.1×10^{-2} molecules site^{-1} s^{-1}. The addition of just 1 mTorr of CO to the hydrogen and ethylene gas mixture results in the cessation of ethane production. Investigation with STM reveals a the presence of large domains of hexagonal surface structure with a periodicity of 12.2 ± 0.3 Å (figure 7b). This structure corresponds to the ($\sqrt{19}\times\sqrt{19}$) R23.4° CO structure reported by Besenbacher et al. [12]. No other ordered surface structure was observed.

4.2.3. *Ethylene hydrogenation and CO poisoning of the catalytic reaction on Rh(111)*

As was the case for Pt(111), the addition of 20 mTorr each of hydrogen and ethylene produce no ordered structures on the Rh(111) surface (figure 8a). The active catalyst was again confirmed using mass spectrometry to detect the production of ethane. The reaction rate was found to be 1.3×10^{-4} molecules site^{-1} s^{-1}. When 2–5.6 mTorr of CO was introduced to the system, the production of ethane stopped completely. STM images

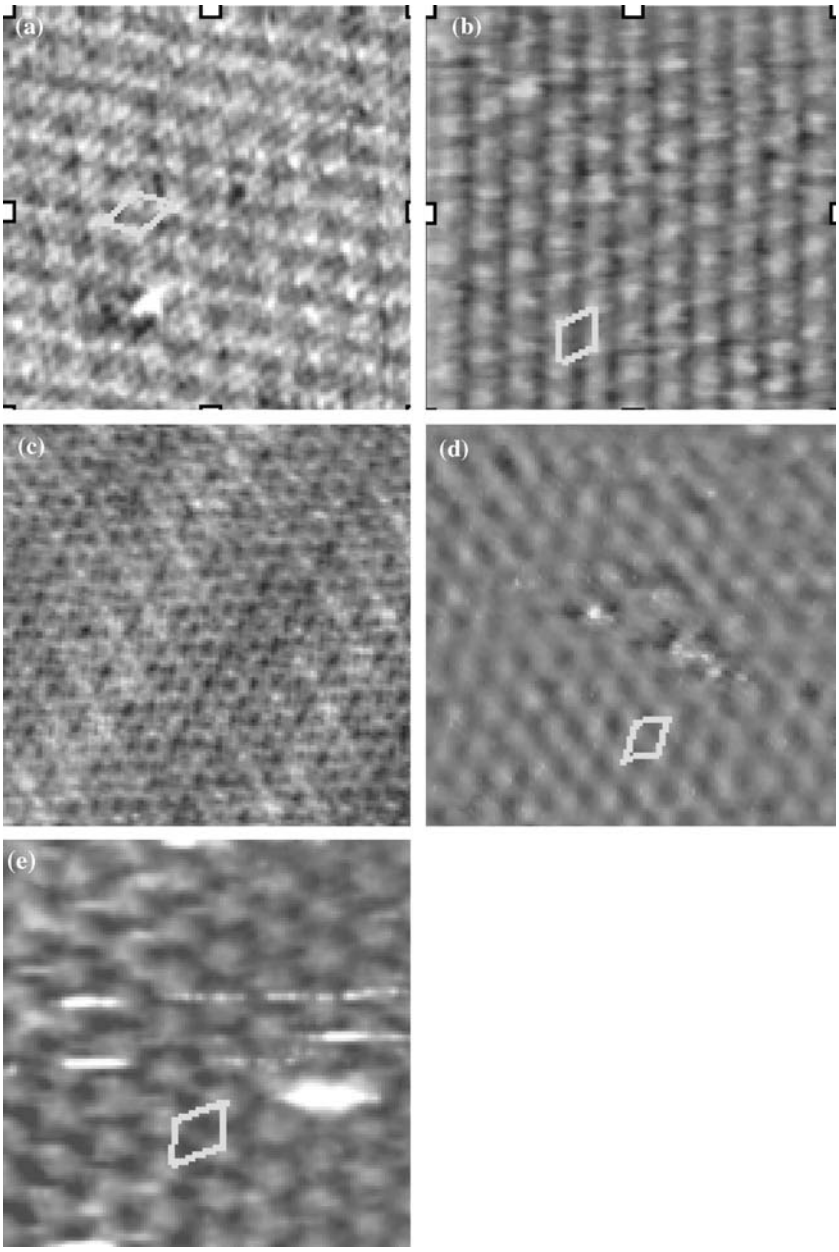

Figure 6. STM images of Pt(111) exposed to low pressure of various cyclic C6 hydrocarbons at 300 K (a) 60 Å×60 Å in the presence of 2×10^{-6} Torr cyclohexane (b) 75 Å×75 Å in the presence of 2×10^{-6} Torr cyclohexene (c) 200 Å×200 Å in the presence of 1×10^{-5} Torr 1,4-cyclohexadiene (d) 100 Å×100 Å in the presence of 1×10^{-5} Torr 1,3-cyclohexadiene (e) 80 Å×80 Å in the presence of 1.2×10^{-5} Torr benzene.

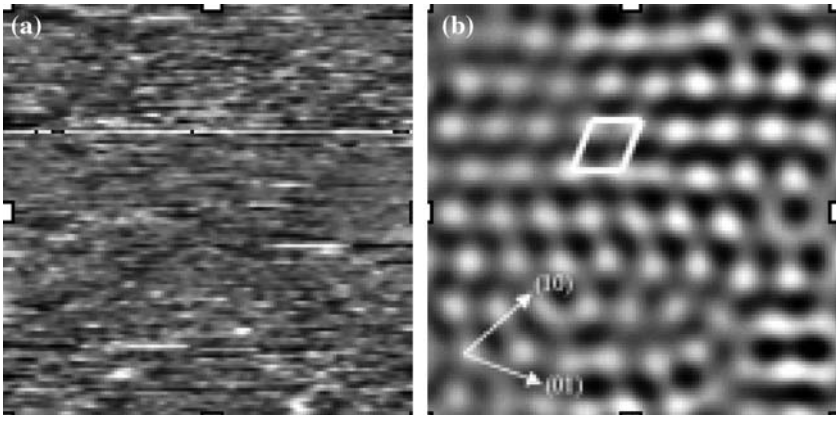

Figure 7. (100×100) $Å^2$ STM images of the Pt(111) (a) exposed to 20 mTorr H_2 and 20 mTorr ethylene (b) exposed to 20 mTorr H_2, 20 mTorr ethylene, and 2.5 mTorr CO.

again show an ordered surface consisting of three different types of surface structures. A c(4×2)-CO + C_2H_3 can be observed in figure 8b. Also, observed were (4×2)-CO + 3 C_2H_3 (figure 8c) and a (2×2)-3CO (figure 8d) structures. Figure 8e shows a domain boundary in which all three structures coexist on the same rhodium terrace.

4.2.4. *Catalytic cyclohexene hydrogenation/dehydrogenation and its poisoning with CO on Pt(111)*

Similar studies to those that investigated ethylene hydrogenation were performed on the hydrogenation and dehydrogenation of cyclohexene on Pt(111). Upon adsorption of cyclohexene to the platinum surface at pressures below 1 Torr at 300 K, the molecule quickly undergoes partial dehydrogenation to form the π-allyl species (C_6H_9) [19]. This species is very stable on the surface but has been shown to further dehydrogenate as the temperature is increased above 300 K. At pressures above 1 Torr the most stable surface species is the 1,4 cyclohexadiene molecule. Our STM studies monitor the active and poisoned catalyst surface in both pressure regimes in the presence of hydrogen, at 300–350 K.

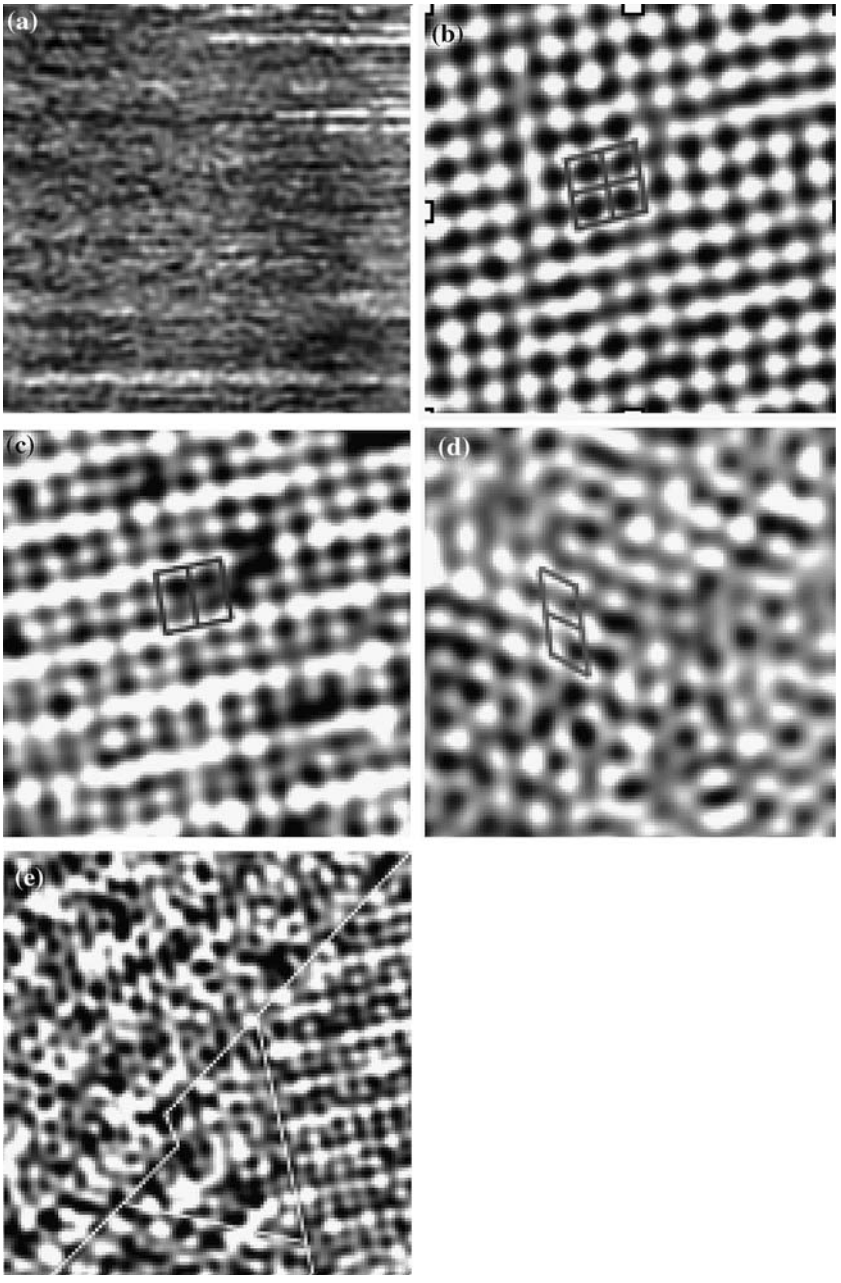

Figure 8. (100×100) Å^2 STM images of Rh(111) (a) exposed to 20 mTorr H_2 and 20 mTorr ethylene (b, c and d) different structures formed in the presence of 20 mTorr H_2, 20 mTorr ethylene, and 5.6 mTorr CO (b) c(4×2)-CO + C_2H_3 (c) (4×2)-CO + $3C_2H_3$ (d) (2×2)-3CO (e) domain boundaries between (2×2), c(4×2), and (4×2) structures, from left to right, respectively.

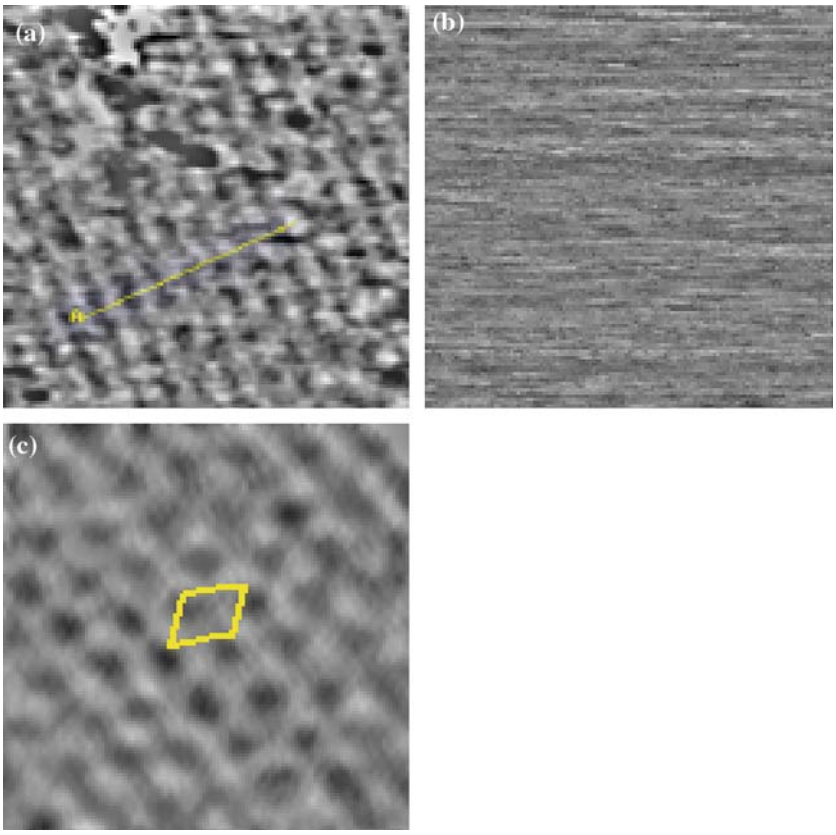

Figure 9. STM images of Pt(111) at 300 K (a) 75 Å×75 Å, 20 mTorr cyclohexene and 20 mTorr H2 added. No catalytic products are detected (b) 50 Å×50 Å, 200 mTorr hydrogen, 20 mTorr cyclohexene added. Catalyst is producing both cyclohexane and cyclohexene. (c) 90 Å×90 Å, 200 mTorr hydrogen, 20 mTorr cyclohexene and 5 mTorr CO. All catalysis has stopped.

The platinum surface in the presence of cyclohexene and hydrogen was studied with STM and mass spectrometry. The surface structure in the presence of 20 mTorr cyclohexene and 20 mTorr of hydrogen at 300 K is shown in figure 9a. The structure that is formed is similar to that formed from pure cyclohexene (figure 6b), indicating that the presence of a 1:1 ratio of hydrogen to cyclohexene is not sufficient to prevent the partial dehydrogenation to the π-allyl. It also does not weaken the adsorbate surface bond sufficiently to prevent imaging. Analysis of bulk gas shows an absence of benzene and cyclohexane indicating an inactive catalyst. Heating the sample to 350 K disorders the surface but still produces no products, suggesting the formation of benzene and other carbonaceous species that are unable to desorb at the given temperature and pressure.

Performing the same experiment using a 10:1 ratio of hydrogen to cyclohexene gives very different results. At room temperature the surface is disordered indicating the high mobility of the adsorbates. Similar to the ethylene experiments the disordered surface also corresponds with an active catalyst surface producing both benzene and cyclohexane (figure 9b). The addition of 5 mTorr of CO poisons the surface and produces the ($\sqrt{19}\times\sqrt{19}$) R23.4° CO structure observed in figure 9c.

When a 10:1 hydrogen to cyclohexene ratio is used but the catalyst temperature is 350 K, again the surface shows no discernable order (figure 10a) while the catalyst produces reaction products. In this case, however, benzene is the major product as has been shown previously [20]. The addition of CO once again deactivates the catalyst, but STM shows no surface structure (figure 10b). As the sample is cooled back down to 325 K the ordering of the CO is restored (figure 10c), suggesting that at 350 K the CO dominated surface is too mobile to image but still poisons by a site blocking mechanism. The experiments were repeated at 300 K using 1.5 Torr of cyclohexene and 15 Torr hydrogen and ultimately the addition of 1 Torr of CO. The results were the same, with the active catalyst surface appearing disordered and the poisoned surface showing clear CO ordering.

5. Conclusions

High pressure/high temperature scanning tunneling microscopy has proven to be an invaluable tool in the investigation of metal surfaces in equilibrium with gas phase species and the study of active catalyst surfaces. STM stands alone in its ability to monitor molecular surface structure at high pressures and its ability to

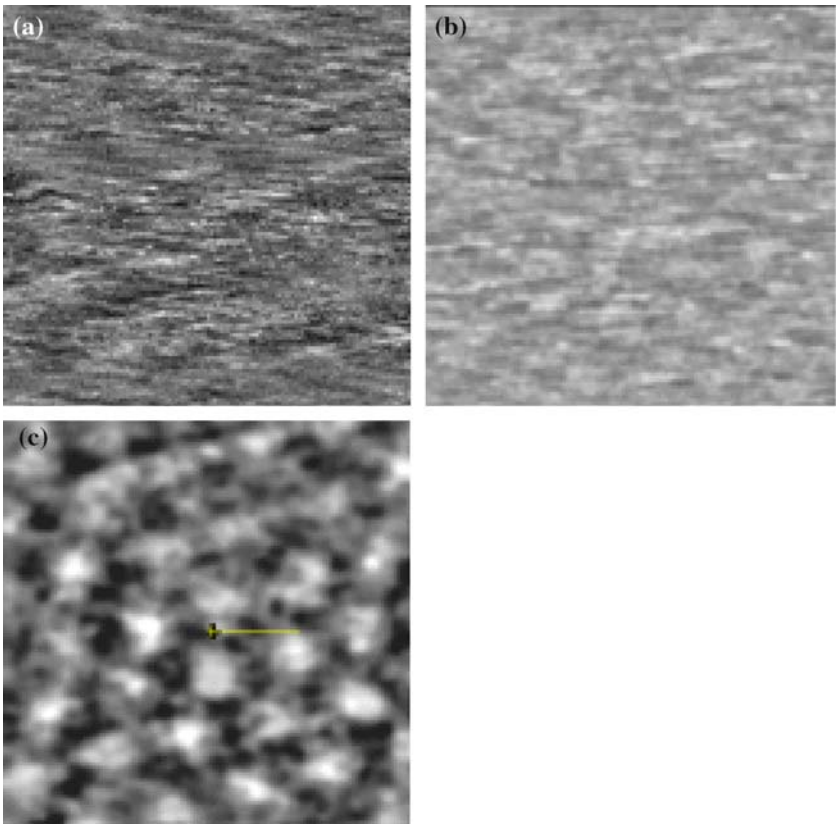

Figure 10. STM images of Pt(111) (a) 100 Å×100 Å image) at 350 K 200 mTorr H2, 20 mTorr of cyclohexene added (b) 95 Å×95 Å image at 350 K, 200 mTorr H2, 20 mTorr of cyclohexene and 5 mTorr CO added (c) 66 Å×66 Å image 200 mTorr H2, 20 mTorr of cyclohexene heated to 350 K, 5 mTorr CO added cooled to 325 K. Surface regains CO ordering.

gather real time molecular information at catalytic conditions. This allows *in situ* monitoring of many industrially important but poorly understood catalytic systems. Our studies have demonstrated both of these properties. In the cases of CO and NO adsorbed individually on Rh(111), and CO adsorbed on Pt(111), new phases were observed that were not present at low pressures. Surface phase diagrams were then constructed as a function of pressure giving insight into the affect of not only adsorbate–substrate interactions but also adsorbate–adsorbate interactions on the surface structures. Coadsorption of NO and CO on Rh(111) has also shown the ability of STM to discriminate between different adsorbates as well as providing dynamic information about site exchange of adsorbates. Finally, our STM studies of adsorption of cyclic C_6 hydrocarbons to Pt(111) has confirmed spectroscopic results concerning surface species, as well as discovered new surface structures.

Catalytic studies we have performed have shown the importance of the mobility of the adsorbed monolayer to catalytic activity. Ethylene hydrogenation on Rh(111) and Pt(111) as well as cyclohexene hydrogenation/dehydrogenation on Pt(111) at several temperatures and pressures were studied. In each system the adsorbed monolayer on catalytically active surfaces was too mobile to image with our STM. In contrast, the formation of an immobile surface overlayer always corresponded to an inactive catalyst. Only in the case of cyclohexene hydrogenation/dehydrogenation on Pt(111) poisoned by CO at 350 K was a mobile surface catalytically inactive. In this case a CO dominated but fairly mobile surface was proposed, that poisoned via site blocking.

The studies we have performed in our laboratory over the last decade have yielded valuable data on their own, but equally as important, they have demonstrated the power and potential of STM as a tool in the study of high pressure systems not accessible to other techniques. As the next generation of higher pressure and temperature STM systems are developed, we can expect even more exciting and surprising discoveries in the years to come.

Acknowledgements

We are grateful to Dr. Miquel Salmeron for many helpful discussions. This work was supported by the Director, Office of Energy research, Office of Basic Energy Sciences, and Materials Science Division, of the US Department of Energy under Contract No. DE-AC02-05CH11231.

References

[1] R.J. Koestner, M.A. Van Hove and G.A. Somorjai, Surf. Sci. 107 (1981) 439.
[2] M.A. Van Hove, R.J. Koestner and G.A. Somorjai, J. Vac. Sci. Technol. 20(3) (1982) 886.
[3] B.M. DeKoven, S.H. Overbury and P.C. Stair, Phys. Rev. Lett. 53 (1984) 481.
[4] J.X. Wang, I.K. Robinson, B.M. Ocko and R.R. Adzic, J. Phys. Chem. B 109 (2005) 24.
[5] J.A. Jensen, K.B. Rider, Y. Chen, M. Salmeron and G.A. Somorjai, J. Vac. Sci. 17 (1999) 1080.
[6] D.C. Tang doctoral thesis.
[7.] P. Cernota, K. Rider, H.A. Yoon, M. Salmeron and G.A. Somorjai, Surf. Sci. 445 (2000) 249.
[8] K.B. Rider, K.S. Hwang, M. Salmeron and G.A. Somorjai, Phys. Rev. Lett. 86 (2001) 4330.
[9] I. Zasada, M.A. Van Hove and G.A. Somorjai, Surf. Sci. Lett. 418 (1998) L89.
[10] K.B. Rider, K.S. Hwang, M. Salmeron and G.A. Somorjai, J. Am. Chem. Soc 124 (2002) 5588.
[11] J.A. Jensen, K.B. Rider, M. Salmeron and G.A. Somorjai, Phys. Rev. Lett. 80 (1998) 1228.
[12.] E. Kruse Vestergaard, P. Thostrup, T. An, E. Laesgsgaard, I. Stensgaard, B. Hammer and F. Besenbacher, Phys. Rev. Lett. 88 (2002) 259601.
[13] M. Montano, M.S. Salmeron and G.A. Somorjai, to be published.
[14] W.L. Manner, G.S. Girolami and R.G. Nuzzo, J. Phys. Chem. B 102 (1998) 10295.
[15] F.C. Henn, A.L. Diaz, M.E. Bussell, M.B. Hugenschmidt, M.E. Domagala and C.T. Campbell, J. Phys. Chem. 96 (1992) 5965.
[16] D.C. Tang, K.S. Hwang, M. Salmeron and G.A. Somorjai, J. Phys. Chem. B 108 (2004) 13300.
[17] U. Starke, A. Barbieri, N. Materer, M.A. Van Hove and G.A. Somorjai, Surf. Sci. 286 (1993) 1.
[18] T.A. Land, T. Michely, R.J. Behm, J.C. Hemminger and G. Comsa, J. Chem. Phys. 97 (1992) 6774.
[19] M. Yang, K. Chou and G.A. Somorjai, J. Phys. Chem. 107 (2003) 5267.
[20] K.R. McCrea and G.A. Somorjai, J. Mol. Catal. A 163 (2000) 43.